Geophys. J. R. astr. Soc. (1983) **73**, 489–505

Complex distribution of large thrust and normal fault earthquakes in the Chilean subduction zone

M. Malgrange and R. Madariaga *Département Sciences Physiques de la Terre, Université Paris VII, and Institut de Physique du Globe, Université P. et M. Curie, 4, Place Jussieu, 75230 Paris Cedex 05, France*

Received 1982 October 28; in original form 1982 February 25

Summary. We present the results of a systematic study of events with $M_s > 6$ in northern Chile (20–33°S), for the period between 1963 and 1971. Medium to large earthquakes near the coast of this region are of three types: (1) Interplate events at the interface between the downgoing slab and the overriding South American plate. These events can be very large reaching magnitudes greater than 8. (2) Intra-plate earthquakes 20–30 km inside the downgoing slab. They have fault mechanisms indicating extension along the dip of the slab and may have magnitudes up to 7.5. (3) Less frequent, $M_s \sim 6$ events that occur near the top of the downgoing slab and have thrust mechanisms with an almost horizontal E–W compressional axis. This type of mechanism is very different from that of the events of type 1 which are due to shallow dipping reverse faulting. There is a rotation of about 30° of the compressional axis in the vertical plane between events of types (1) and (3). Three groups of events near 32.5°, 25.5° and 21°S were studied in detail. Depth and mechanisms were redetermined by *P*-wave modelling and relative locations were obtained by a master event technique. Near 32.5°S, only events of types 1 and 2 were found in the time period of this study. At the two other sites, the three types of events were identified. This shows clearly that there are compressive stresses at the top of the slab and extension at the centre, a situation which is usually found in the areas where a double Benioff-zone has been identified in the seismicity.

Introduction

The general features of the seismicity associated with oceanic plate subduction were established by Isacks, Oliver & Sykes (1968). Recent detailed studies of seismicity and focal mechanisms have revealed important regional variations in the mode of subduction; for example, there are large variations in the angle of the Wadati-Benioff zone, different degrees of coupling between the plates, etc. (Isacks & Barazangi 1977; Uyeda & Kanamori 1979). In this context, the seismicity of the South American subduction zone has been the subject of renewed interest in recent years. Some early observations by Kausel & Lomnitz (1968), have been extensively documented by Barazangi & Isacks (1976), Isacks & Barazangi (1977) and Hanus & Vanek (1978). They showed that the Peru–Chile subduction zone is segmented along its length with Wadati–Benioff zones of variable dip. Source mechanisms for medium to large sized earthquakes were studied by Stauder (1973, 1975). Most of the Chilean coast is subjected to more or less periodically recurrent great earthquakes with magnitude greater than 8 (Lomnitz 1970; Kelleher 1972). In the time lapse between these great events an important activity of large earthquakes with $6.0 < M_W < 7.5$ takes place near the Chilean coast. In a recent paper (Malgrange, Deschamps & Madariaga 1981) we showed that two large, destructive earthquakes ($M_S = 7.5$) that occurred near Valparaiso on 1965 March 28 and 1971 July 9 had very distinct depths and mechanisms. The former shock was a normal fault event that took place clearly inside the subducted plate, while the second one was a shallower thrust event at the interface between the two plates. From a re-examination of Stauder's (1973) fault plane solutions we found a number of events that, although having almost the same epicentral coordinates, had very different focal depths; normal fault events seemed to occur systematically deeper than thrust earthquakes (Fig. 1). These observations seem to indicate a complex state of stress in the downgoing slab somewhat reminiscent of the double layer found in Japan by Hasegawa, Umino & Takagi (1978). However, in a study

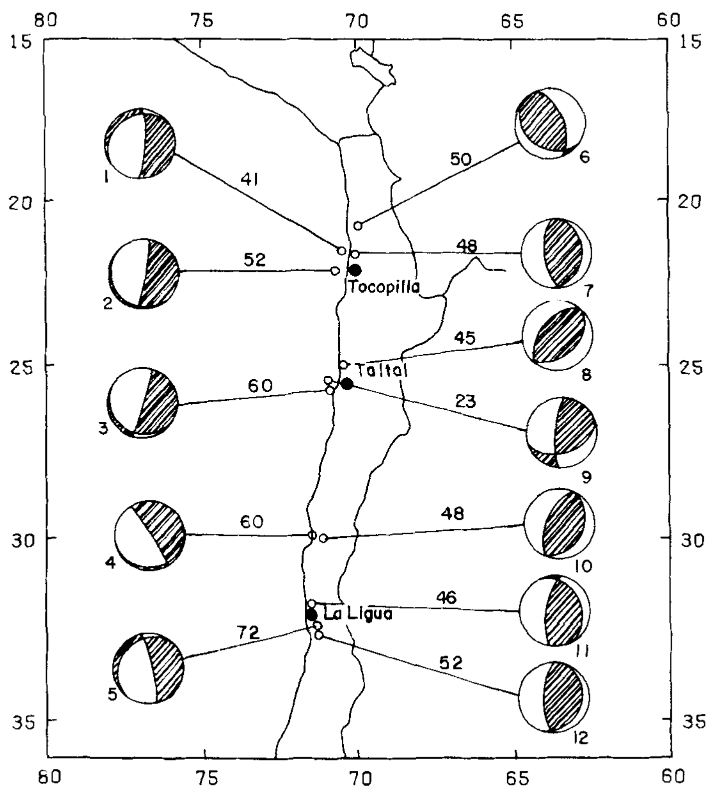

Figure 1. Selected earthquakes near the coast of northern Chile. The events on the right are all interplate underthrust earthquakes, except numbers 6 and 8 which are compressional shocks that occurred on the top of the downgoing slab. The redetermined depth of the earthquakes in kilometres is indicated by the number on top of the lines joining the focal spheres to the epicentres (open circles). Filled circles indicate the location of the cities referred to in the text. Cross-hatched quadrants denote compressional first motion.

of these double Benioff zones, Fujita & Kanamori (1981) classified the Chilean subduction zone as a young and fast one, without a double zone.

The purpose of the present paper is to report on some results we have obtained from the study of a number of selected events in North-Central Chile. We use body wave modelling to determine depth and improved fault plane solutions. Relative location is then used to find the spatial arrangement of the different groups of events. With these techniques we study two groups of earthquakes: one near 25°S near the town of Taltal where a large earthquake occurred in 1966 (Deschamps, Lyon-Caen & Madariaga 1980). The other group was located near 21°S, close to the city of Tocopilla. Together with the study of the earthquakes near Valparaiso, our results demonstrate a diversity of source mechanisms, suggesting a very complex state of stress in the Nazca–South American plate interface.

Method

We tried to determine simultaneously improved fault plane solutions and hypocentral depths by means of long-period *P*-wave modelling. Fault plane solutions for South American earthquakes are usually rather poorly constrained because of the lack of stations to the west of the epicentre; the same problem affects the hypocentral depths. The data we use are selected WWSSN long-period *P*-wave recordings. The vertical components of the observed records were digitized at 0.5 s time steps and were brought to a common amplification (usually 1500). No filtering was applied to these data. In order to avoid problems with upper mantle triplications and diffraction by the mantle–core boundary only data from distances between 30° and 90° were used.

For the modelling we used simple ray theory from a double couple source. This technique has been thoroughly described by Helmberger & Langston (1975), Kanamori & Stewart (1976) and, in the particular version used here, by Deschamps *et al.* (1980). We included the free surface reflected phases *pP* and *sP* calculated for a homogeneous half-space model of the source area. Since all our events are in the upper mantle we adopted a mean *P*-wave velocity above the source of 7.5 km s^{-1} and an *S*-wave velocity of 4.5 km s^{-1}. Lack of crustal and upper mantle structure of the source region prevented us from using a more realistic model of the medium above the source. Tests made with a simple crust over a half-space model did not show major differences with the synthetics calculated here (Malgrange *et al.* 1981). Attenuation in the mantle was incorporated by means of Futterman's operator with $T/Q = 1$ for *P*-waves. Starting with the fault plane solution obtained from first motions and the hypocentral depth reported by ISC, we determined the source time function by visual fit of the observed and synthetic records. Since most of the earthquakes studied were relatively small with source time functions of duration shorter than 5 s, only the width of the source function could be determined and we used simple trapezoidal impulses. For the larger events we used modified trapezoids designed to fit the data as closely as possible. The same source time function was used for *P*, *pP* and *sP* waves, although it is well known that the *sP* source functions usually have a longer duration than the *P* pulses (Hanks 1981). Our observations do not have enough resolution to detect such fine details.

Once the source time function was adopted we proceeded to determine the hypocentral depth. Except for the largest shallow events, there was none of the usual trade off between depth and source time duration of shallow focus shocks. Depth was very well constrained by the delay between *P* and *pP* or *sP*. Finally, the fault plane orientation was modified in order to fit the relative amplitudes of the direct and reflected phases, and the polarities in the original solution. The seismic moment was finally calculated from the best fitting model. The main source of error in the preceding approach is in the half-space model assumed for the source area. The depth determined in the modelling depends on the velocity in the half-space and may be subject to some variation since the *P*-wave velocity of 7.5 km s^{-1} is only a representative average of the velocity above the source.

The *P*-wave modelling provides information about the depth of the events considered. In order to get an idea of the relative location of the events in space we relocated them by means of a master-event technique. We took one event as fixed and then located the others with respect to it. We then checked the overall consistency of the results choosing another event as the master and repeating the relative location. The method is closely related to the one described by Fitch (1975) and Spence (1980).

The Taltal Group (25°S)

The first group of earthquakes that we shall discuss was located in northern Chile at the limit between the 30° dipping North Chile segment of the Benioff zone and the shallower dipping North-Central Chile segment. The seismicity in this area was studied by Stauder (1973) and Hanus & Vanek (1978) who showed that the intermediate depth seismicity stops at around 100 km depth between 25 and 28°S, while it penetrates down to 300 km in the adjoining areas.

This group comprises three events, the largest being the 1966 December 28 earthquake (9 in Fig. 1) which is a large shallow thrust event. Then, there is the 1965 February 23, $M = 6.9$, earthquake (3 in Fig. 1), which is a normal fault intraplate event. Finally, the smaller event of 1967 June 21 (8 in Fig. 1) is a thrust event with a very different mechanism from the under-thrust earthquakes associated with the subduction of the Nazca plate.

THE 1966 DECEMBER 28 EARTHQUAKE

This earthquake was studied in detail by Deschamps *et al.* (1980) who showed that it was a typical subduction zone earthquake. Its mechanism (9 in Fig. 1) was determined from first motions, *P*-wave modelling and long-period surface waves. It is a shallow underthrust event with dip of 41° and a rather important strike-slip component. From the amplitude of long-period surface waves, the seismic moment was calculated as $M_0 = 4.5 \times 10^{20}$ Nm. From the *P*-wave modelling a somewhat smaller moment (3.4×10^{20} Nm) was obtained. These and other parameters for this event are listed on Table 2. Further details may be found in Deschamps *et al.* (1980).

THE 1965 FEBRUARY 23 EARTHQUAKE

Focal mechanisms for this event were proposed by Isacks & Molnar (1971) and by Stauder (1973) who used both long-period *P* first motions and *S*-waves polarizations. As is common for intermediate depth, normal fault events under the Chilean coast, one finds a very well constrained, almost vertical fault plane. North American stations record dilatations TRN and SBA are almost nodal and fix the azimuth of the vertical fault plane. The European stations (PTO, MAL, GRM) limit the dip angle between 82°E (Stauder's 1973 solution) and 90°E (Isacks & Molnar's 1971 result). The second nodal plane is not constrained by *P*-waves and it was determined from *S*-wave polarities.

We read 48 WWSSN records for this earthquake, the solution being in good general agreement Stauder's. Twelve vertical long-period *P*-wave trains were digitized and brought to a common amplification of 1500. Fig. 2 shows the records displayed as a function of azimuth. At the time of this earthquake most WWSSN has a seismometer with a period of 30 s and a

23 Feb 65

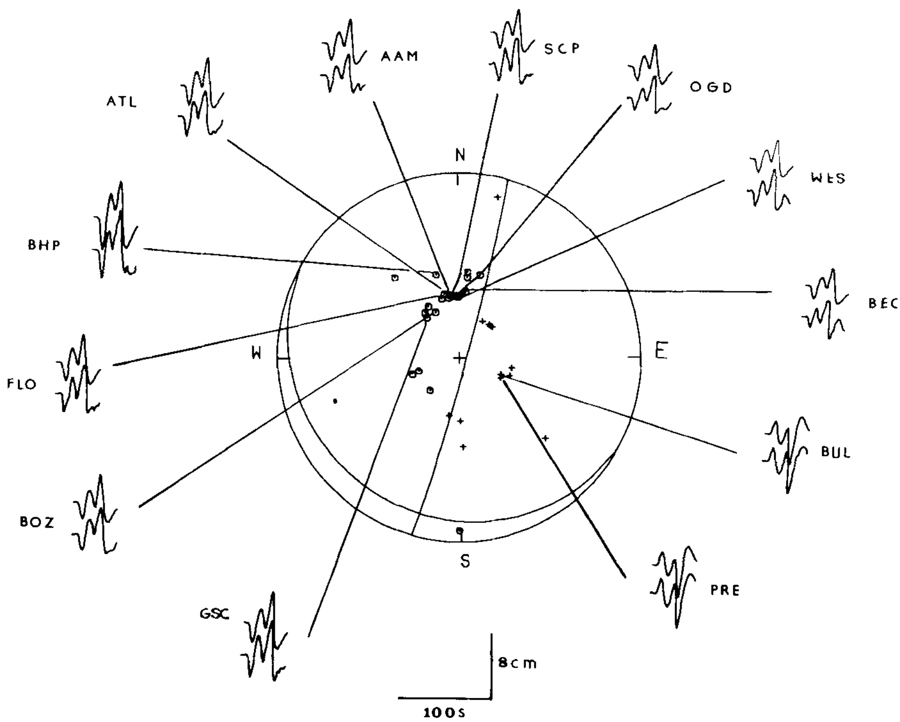

Figure 2. Long-period *P*-wave modelling of WWSSN records of the 1965 February 23 earthquake at stations with distances ranging from 30° to 90°. For every station we show on top the synthetic seismogram and below it, the observed one. All records are normalized to an amplification of 1500.

galvanometer calibrated at 100 s. The synthetics calculated for the source mechanism in Fig. 2 and the source time function of Fig. 10 provide an excellent fit to the observations. Since one fault plane is almost vertical, the *sP*-wave is the largest phase at most of the distant ($30° < \Delta < 90°$) stations. This is the second phase clearly observed in the records shown in Fig. 2. For most of the stations, except PRE and BUL, *pP*-waves are almost nodal. From the modelling we determined a focal depth of 59 km, that is, this earthquake was about 36 km deeper than the 1966 December 28 event. We then attempted to fix the dip of the vertical fault plane more closely. Unfortunately, the observations do not control this dip very well and satisfactory fitting of the observations was obtained for dip angles between 75° and 90°E.

The modelling yields a very simple trapezoidal source function with a width of 5 s. It is difficult to find more details from records obtained with a 30 s seismometer. The seismic moment was determined as 0.35×10^{20} Nm, which was confirmed by a moment tensor inversion (Malgrange 1981).

THE 1967 JUNE 21 EARTHQUAKE

This is a much smaller earthquake ($m_b = 6.7$) situated slightly to the north of the preceding ones. This event presents some particular interest since it has a compressive mechanism which is not of the shallow thrust type typical of subduction zones. A fault plane solution determined from *P*- and *S*-wave polarities was proposed by Stauder (1973). The nodal planes were poorly constrained with compressions at all stations except at ANT and LPB. From the *S* polarities two nodal planes striking NE–SW and an almost horizontal NW–SE compressional axis were found.

Most of the *P*-wave recordings for this event had low signal-to-noise ratios. Ten records were finally selected and digitized; they are plotted in Fig. 3. The source time function is very short, with a total duration of 4 s as shown in Fig. 10. This is practically a delta function for the long-period WWSSN stations. Very clear *pP*- and *sP*-waves are observed at most stations. The *pP* phase is particularly clear at the CAR station, which is very well reproduced by the synthetic record. The depth calculated from the modelling is 45 km for the simple model of the structure that we are using; it is much greater than that determined by ISC (23 km). We could not find any reasonable values of the *P*-wave velocity for which we could fit the observations at this depth. In all these cases the separation between direct and reflected phases was too short and the synthetics had too short a total duration compared to the observations. On the basis of the ISC depth Stauder (1973) proposed that this event took place in the South American plate. Our result indicates that this event is well inside the subducted oceanic plate. The preferred focal parameters are listed in Table 2. From the modelling we estimate that the azimuth and dip of the NW dipping plane are constrained to within 3° and the slip angle to 5°. The seismic moment was found as 2.3×10^{18} Nm.

In order to determine the complete spatial arrangement of these earthquakes we then proceeded to relocate them. We took the 1966 December 28 earthquake as the master event and located the other two with respect to it. The 1965 February 23 earthquake was found

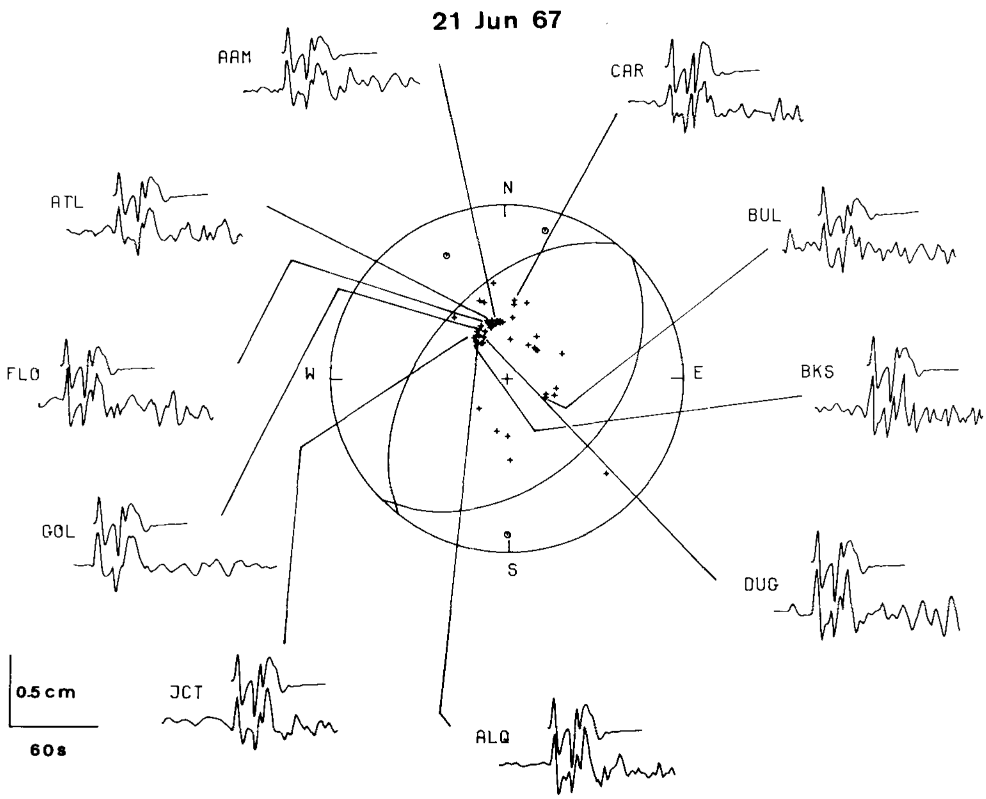

Figure 3. Modelling of *P*-waves for the earthquake of 1967 June 21 in the Taltal area of northern Chile. Records normalized to amplification of 1500.

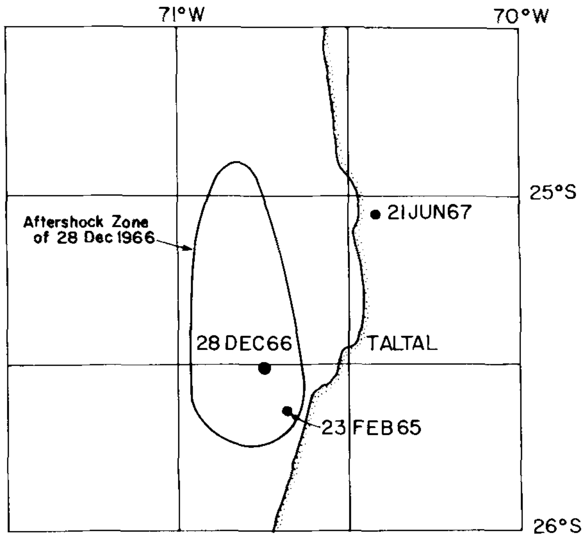

Figure 4. The Taltal area with the epicentral location of the three events studied in the text. We also indicate the aftershock zone of the large 1966 December 28 earthquake as determined from a portable network by Pitt & Ellis (1968).

to have almost the same epicentral coordinates as the master event. Since the 1966 event has a source area of about 40 x 80 km (Pitt & Ellis 1968), this shows that the 1965 event is an intra-oceanic plate, normal fault event occurring some 35 km below the interface between the oceanic and continental plates. Then we relocated the 1967 June 21 earthquake. Clear azimuthal variations of the arrival time differences between this event and those of 1966 and 1965 were detected. In order to check the consistency of the arrival times we relocated the 1967 event with respect to both the 1966 and the 1965 ones. The results are consistent within the error of the relocation method. The 1967 event was located 70 km to the north of the 1965 event as shown in the map of Fig. 4. We are confident that the 1967 event took place inside the oceanic plate some 20 km below the hypocentre of the 1966 earthquake. It is a compressive event with an almost horizontal axis of compression. Its location with respect to the 1965 event is suggestive of the double layer observed in North Nonshu (Japan).

The Tocopilla (21° S) group

There are four earthquakes in this group situated along the Chilean coast between 21° S and 22° S. These events are of particular interest since they occurred inside the important gap of great earthquakes of northern Chile and southern Peru (Kelleher 1972; McCann *et al.* 1979). The earthquake of 1967 December 21 is the largest to have occurred inside this gap (7 in Fig. 1) in the last 50 years.

We shall also study two other smaller events: number 2 on 1970 June 19, a normal fault earthquake some 65 km to the south of the 1967 December one, and event number 6 about 60 km to the north of 1967 shocks.

THE 1967 DECEMBER 21 EARTHQUAKE

This is the largest event of the group, it has a shallow thrust mechanism determined by Stauder (1973) for which only one dilatation was observed at the NNA station. The focal mechanism has a N–S plane dipping steeply to the west. The second fault plane is shallow ($\delta = 28°$) but poorly constrained. Stauder (1973) fixed this second plane with the help of the polarization of *S*-waves, this is the solution used in the modelling shown in Fig. 5. The time duration of the rupture process is well constrained by the width of the first peak. We find a total source time duration of 10 s. The separation between the positive peaks in Fig. 5 is controlled by the source depth. This depth is definitely larger than the 33 km determined by ISC. With the simple model of the structure that we are using here, we find a depth of 46–48 km. All long-period *P*-wave records shown in Fig. 5 show a clear second arrival about 12 s after the first one, in the same direction as the first motion. It could be interpreted as a reflected phase but we observe an azimuthal dependence of the arrival time of this secondary impulse. It arrives later at the stations VAL and GRM located to the east of the source. For this reason, we interpret it as being due to the source complexity. Assuming that the second shock has the same source mechanism as the first one, we found the source time function shown in Fig. 10 and determined a seismic moment of $M_0 = 1.43 \times 10^{20}$ Nm. This is a rather large event which could naturally be associated with the subduction of the Nazca plate. There are, however, two observations that complicate its interpretation. The depth that we determined is on the order of 46–47 km; even if the model used were substantially modified this depth could hardly be made shallower than 40 km. This depth seems too deep for the interface between the oceanic and continental plates under the Chilean coast line. Another interesting aspect of this earthquake is that it had very few aftershocks located by ISC. In Fig. 9 we present the area around Tocopilla and the epicentres of all the events reported by

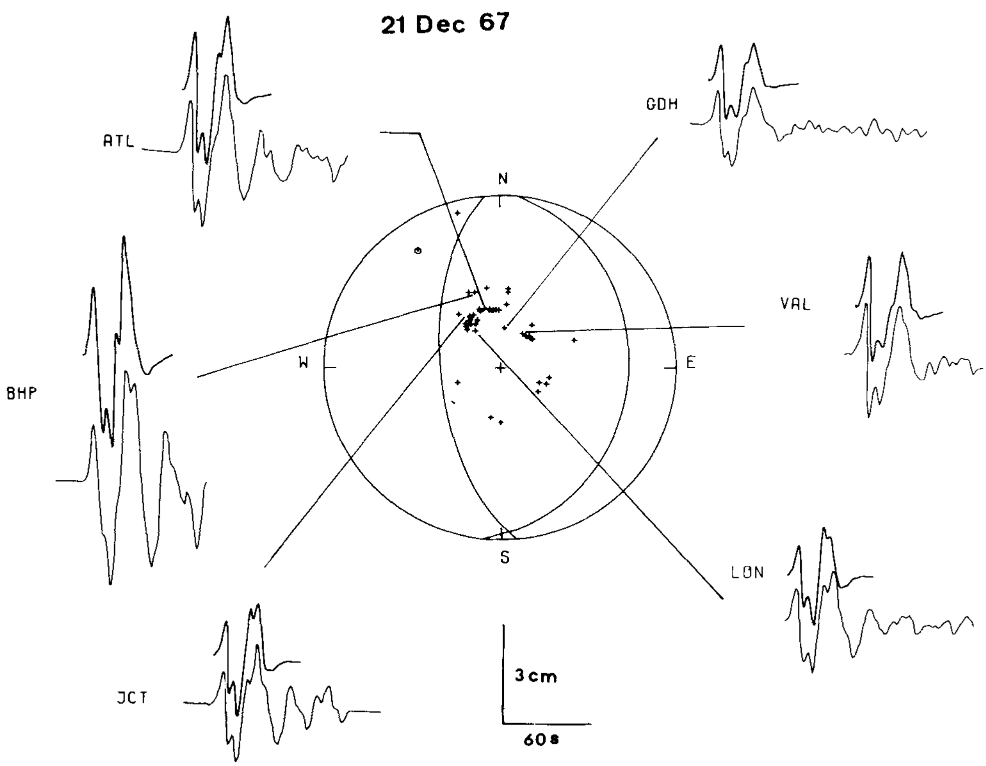

Figure 5. Long period *P*-wave modelling of the WWSSN recordings of the 1967 December 21 earthquake. For every station we show at the top the synthetic seismogram and at the bottom, the observed one. All records were brought to a common amplification of 1500.

ISC for the period immediately following the earthquake until 1968 January. Compared to other interplate earthquakes of its size that we have studied along the Chilean coast, this earthquake has a very small number of aftershocks. In this sense it is much closer to the large intraplate earthquake of 1965 March 28 near Valparaiso studied by Malgrange *et al.* (1981).

THE 1967 DECEMBER 25 EARTHQUAKE

This is the principal aftershock of the December 21 earthquake. The focal mechanism (Fig. 6) shows a relatively well constrained almost vertical N–S plane. The Peruvian stations ARE and NNA as well as the European ones are almost nodal. As may be seen in the observed records shown in Fig. 6, the *P*-waves are rather complex. From an analysis of the amplitudes and relative arrival time of reflected phases we found that the second positive peak is due to the *sP*-wave. The synthetic seismograms shown on Fig. 6, above the observed ones, were calculated for the inferred source depth of 41 km. This depth is closely controlled by the four peaks observed in all the North American stations. The source time function shown in Fig. 10 is a simple trapezoid of mean width 3 s.

In all the American stations there appears to be a clear secondary arrival about 18 s after the *sP*-wave. Such a long delay may not be due to reflection and is probably due to source complexity. We have not tried to model this secondary arrival.

Finally, we modified the fault plane solution proposed by Stauder (1973) in order to fit simultaneously the *P*-wave observations and the first motions at PEL and SOM. The

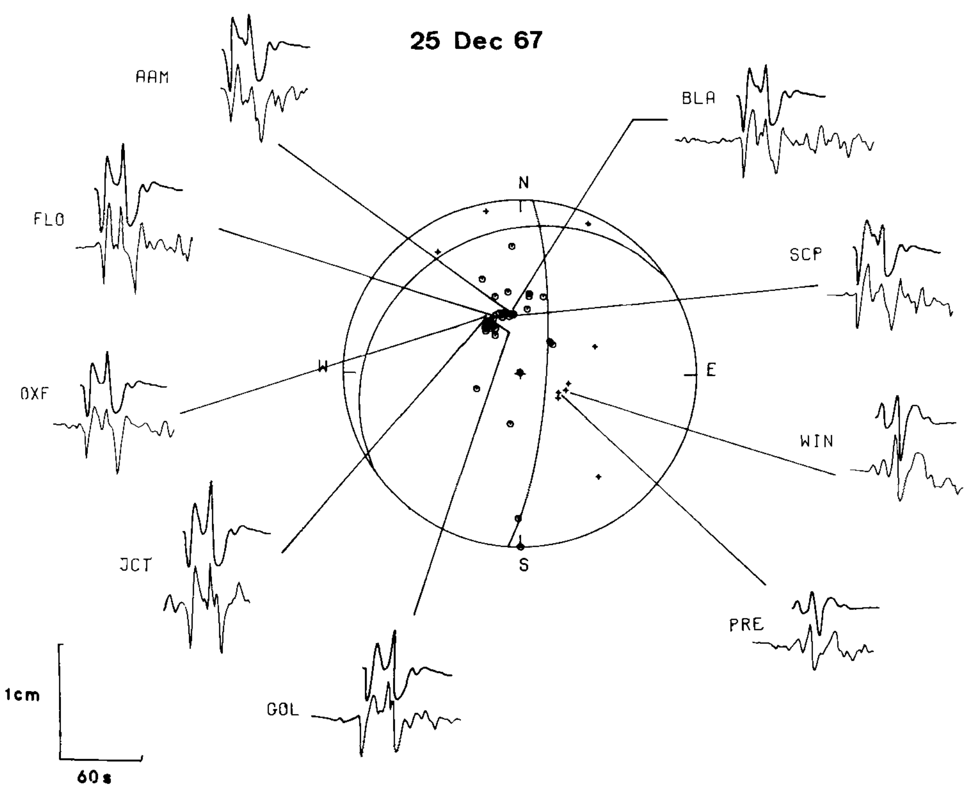

Figure 6. Modelling of *P*-waves for the earthquake on 1967 December 25 in the Tocopilla area of northern Chile.

proposed solution accounts well for the difference in wave form observed in North America and in South Africa. The seismic moment for this earthquake was $M_0 = 4.3 \times 10^{18}$ Nm, the other parameters being listed on Table 2. Our results show that this aftershock has a different mechanism from that of the main shock of December 21.

THE 1970 JUNE 19 EARTHQUAKE

This earthquake presents many similarities with the 1967 December 25 aftershock although it is somewhat larger. In both cases the *P*-wave polarities determine a nearly vertical N–S fault plane dipping steeply to the east. European stations as well as TRN and PDA are very nodal. On the other hand, the South African stations have larger *P* amplitudes and they may not be as nodal as implied by Stauder's (1973) mechanism. For this reason we modified his mechanism as shown in Fig. 7. This earthquake was very well recorded and in Fig. 7 we show nine long-period WWSSN *P*-wave records that we attempted to model. Waveforms are very similar to those of the 1967 December 25 aftershock. Synthetic *P*-waves were calculated for a simple half-space model and for a model with a crustal layer 33 km deep over a half space. Both give a focal depth of 52 km which is practically the same as given by ISC. The source time function used in generating the synthetics is a simple trapezoid of mean width 4 s as shown in Fig. 10. From the *P*-wave modelling we deduce a seismic moment $M_0 = 7.3 \times 10^{18}$ Nm and the other source parameters are shown in Table 2.

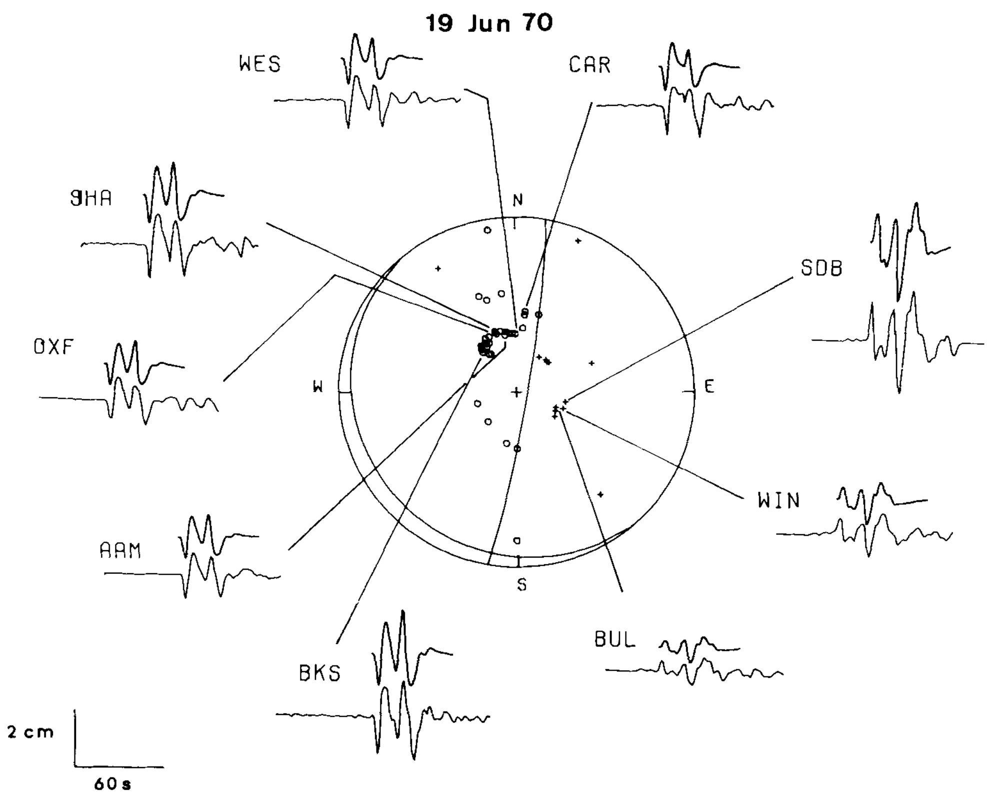

Figure 7. Modelling of *P*-waves for the earthquake of 1970 June 19.

THE 1970 DECEMBER 28 EARTHQUAKE

With those of 1967 June 21 and 1969 November 15 this earthquake was identified by Stauder (1973) as a shallow intra-continental plate reverse fault shock. An examination of the records of this earthquake showed, however, that its depth was substantially deeper than reported by ISC. The fault plane solution proposed by Stauder (1973) had to be modified because it was not compatible with the observations of a clear dilatation at LPB and a clear compression at ARE. Also PEL and ANT present dilatations which were not incorporated in Stauder's mechanism. Using all the data available we came up with the fault plane solution shown in Fig. 8 which we used for the modelling of *P*-waves. This is a rather small event and most *P*-wave observations had low signal-to-noise ratios but we could recover a number of good quality observations. As shown in Fig. 8, the *P*, *pP* and *sP* are clearly visible at most stations, which constrain very well the depth of the earthquake. With the simple half-space model we find a focal depth of 50 km, much deeper than what was reported by ISC. This depth places the shock definitely inside the downgoing slab. The good agreement between observed and synthetic records confirms that the source mechanism was a reverse fault. The source time function for this event has a width of about 3 s and we find a seismic moment of 9×10^{17} Nm.

RELOCATION OF THE TOCOPILLA EARTHQUAKES

We relocated, with respect to the 1967 December 21 earthquake, the largest shock in the group. The 1967 December 25 aftershock is clearly located at almost the same latitude, some

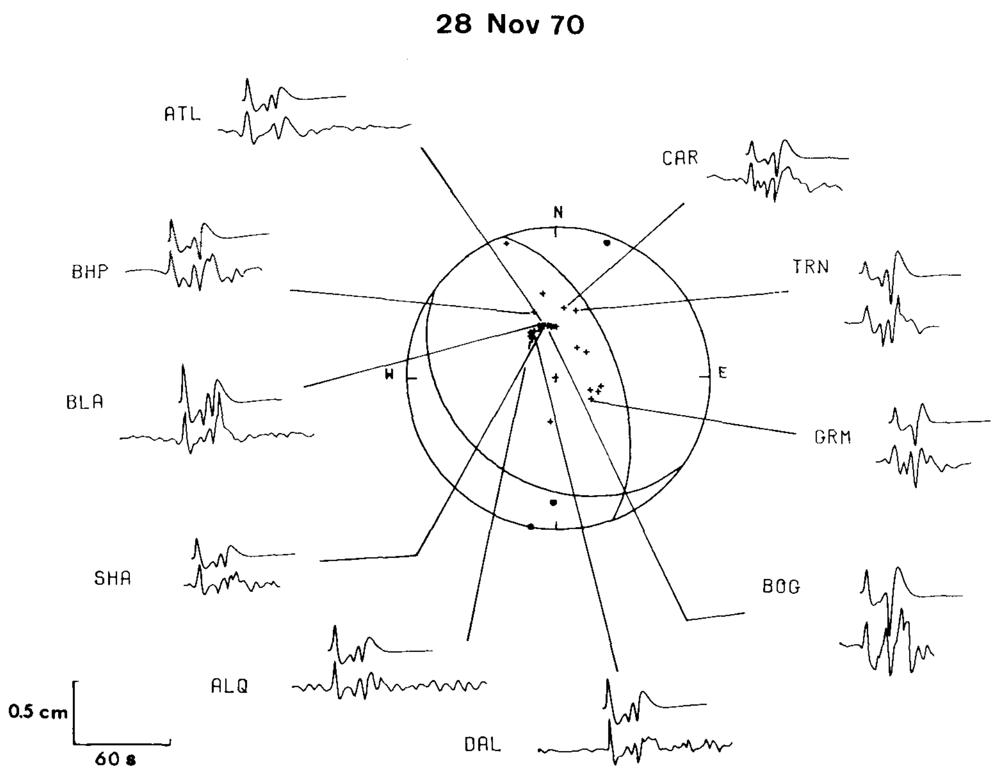

Figure 8. Modelling of *P*-waves for the earthquake of 1970 November 28.

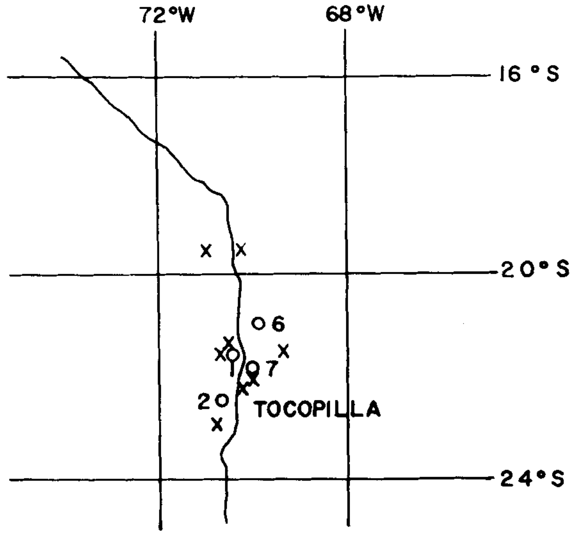

Figure 9. The Tocopilla area of northern Chile. The circles indicate the earthquakes studied in this paper and the numbers refer to Table 1. The crosses indicate the location of the aftershocks of the 1967 December 21 earthquake located by ISC These are all the events in this area from December 21 until the end of 1968 January.

60 km NW of the reference event (see Fig. 9). The other earthquakes were similarly relocated with respect to the large event of 1967 December 21. The 1970 June 19 normal fault event is clearly to the south of the source area of 1967 December and oceanwards of the reference event. Finally, we located the small event of 1970 November 28; this is an almost 45° reverse fault earthquake. After relocation we found that it was located about 100 km north of the 1967 December events.

The relocation shows that the two normal fault events (1 and 2) are located oceanward from the large underthrust earthquake of 1967. The latter is well located by ISC; this location may be verified from the isoseismal map prepared by the Department of Geophysics (University of Chile). Unfortunately there are no local stations in this area closer than 100 km and we have no instrumental way of improving the absolute locations. The situation is different here from that near Taltal or Aconcagua (Malgrange *et al.* 1981), where the normal fault event occurs below and deeper than the overthrust events. Here the normal fault shocks have the same depth and are clearly oceanward of the thrust events.

Other events

As seen in Fig. 1, there are two other groups where normal and thrust faulting was observed very close to the Chilean coast. The southernmost group, near 32.5°S, was studied in detail by Malgrange *et al.* (1981). Two large events on 1971 July 8 and 1965 March 28 occurred at almost the same place but while the former had a typical thrust mechanism associated with subduction, the latter was an intra-plate extensional event. Fault mechanisms and depth were determined from surface and body wave modelling. The results we obtained are listed in Table 2. We also studied a smaller event in this area that appeared as a foreshock of the March 28 event. This earthquake, also listed in Tables 1 and 2, is much smaller than the other two and is an interplate earthquake about 50 km north of the two bigger events.

Table 1. Location of the earthquakes studied in this paper.

No.	Date	Time	Latitude (°S)	Longitude (°W)	Depth	M_S
1	1967 Dec. 25	10:41	21.54	70.55	41	5.8
2	1970 June 19	10:56	22.27	70.72	52	6.2
6	1970 Nov. 28	11:08	20.97	70.05	50	6.0
7	1967 Dec. 21	02:25	21.9	70.1	48	6.3
3	1965 Feb. 23	22:11	25.67	70.79	60	6.2
8	1967 June 21	20:09	25.08	70.45	45	5.7
9	1966 Dec. 28	08:19	25.51	70.74	23	6.9
4	1963 Mar. 10	10:51	30.0	71.2	60*	6.3
10	1967 Sep. 26	16:11	30.0	71.5	48	6.0
5	1965 Mar. 25	16:33	32.4	71.2	72	6.4
11	1965 Mar. 22	22:56	31.9	71.5	46	6.0
12	1971 July 9	03:03	32.5	71.2	42	6.6

*ISC depth. Earthquake not studied by us.

There is another group, near 30°5, containing events numbers 4 and 10 in Fig. 1. Unfortunately, event number 4 of 1963 March 10 took place before the complete establishment of the WWSSN stations and we could not study it more carefully. The event of 1967 September 26 was modelled by the technique used for all the other events in this paper. The details of the modelling are reported in Malgrange (1981). We find a depth of about 48 km and a fault plane dipping at 25° to the SE. This event is very similar to the earthquake of 1967 June 21 in the Taltal area. Although its interpretation is ambiguous since we lack additional data, we suggest that it is probably a compressive event inside the downgoing slab.

Source parameters

From the *P*-wave modelling we have obtained very good estimates of the seismic moments of the events in this paper. The fitting of the *P*-waves yields the source time functions which are shown in Fig. 10. For the smaller events simple trapezoids were used and we feel that only two parameters are well determined: the area of the far field pulse which is proportional to the seismic moment, and the pulse width or duration. These two parameters together with

Table 2. Source parameters.

No.	Date	Source duration (s)	M_0 (10^{20} Nm)	M_W	$\Delta\sigma$ (MPa)	ϕ (°)	δ (°)	λ (°)
1	1967 Dec. 25	3	0.043	6.4		4–10	78	−104
2	1970 June 19	4	0.073	6.5		10	85	−85
6	1970 Nov. 28	1	0.009	6.0		340	58	105
7	1967 Dec. 21	7	1.430	7.4	4.8	6	28	100
3	1965 Feb. 23	5	0.35	7.0		16	86	−78
8	1967 June 21	2	0.023	6.2		40	46	94
9	1966 Dec. 28	13	4.0	7.7	7.3	70	41	150
10	1967 Sep. 26	2	0.048	6.4		25	32	85
5	1965 Mar. 28	8	1–1.8	7.5	9.1	348	80	−100
11	1965 Mar. 22	1	0.04	6.4		191	70	106
12	1971 July 9	16	5.6	7.8	3.8	180	66	87

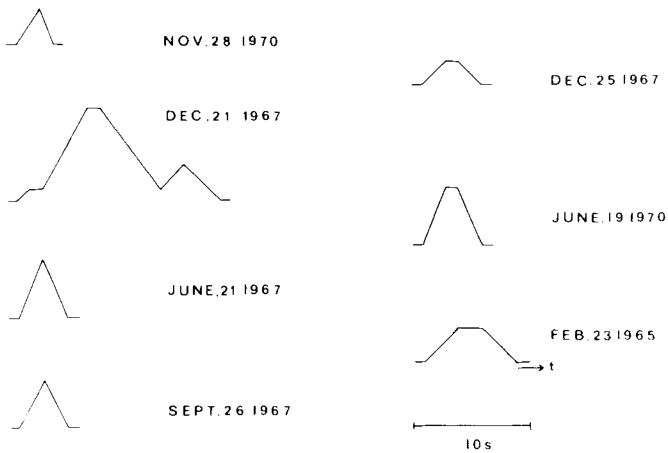

Figure 10. The source time functions used in generating the synthetic seismograms for all the events considered in this paper. Amplitudes are indicative only since these source pulses are normalized by the seismic moment.

the fault plane angles are listed in Table 2. We have also calculated the moment magnitude M after Kanamori (1977) and listed it in this table.

We did not attempt to determine stress drops for the smaller events. For the largest ones, the stress drop was calculated by Deschamps *et al.* (1980) for the large Taltal earthquake of 1966 December 28; and by Malgrange *et al.* (1981) for the two large events in Aconcagua (1965 March 28 and 1971 July 8). For the large event of 1967 December 21 we calculated the stress drop as follows: since this event had very few aftershocks we determined the source radius, r, assuming a circular source. From the approximate relationship $T = 2r/\beta$ where $T = 10$ s is the mean source duration determined from Fig. 12, we find a radius of $r = 23$ km for a shear velocity of 4.5 km s^{-1}. Using the circular model, and the standard relationship between moment, stress drop and source radius we find a stress drop of 48 bar = 4.8 MPa. This value is subjected to a rather large uncertainty because of the way the source area was estimated. A similar procedure was used for the 1965 February 22. It is interesting to note the stress drops found for all the large earthquakes are rather high, ranging from 38 to 91 bar.

Discussion

Several recent studies of seismicity and source mechanism have shown that there are large variations in the stress regimes of different subduction zones (Fujita & Kanamori 1981). These differences appear to correlate with the age and velocity of the subducted plate, the presence of marginal basins, etc. The Chilean subduction zone is a fast and young one in the classification established by Fujita and Kanamori, without a double Benioff zone. We should then have the usual shallow underthrust events at the interface between the plates, and extensional intermediate depth events due to slab pull (Isacks & Molnar 1971).

The results reported in this paper show a more complex situation, with compressional events near the top of the downgoing slab and normal fault events oceanwards of the main underthrust earthquakes. Our results are synthesized in Fig. 1 where we show the geographical locations of the events, their depths and mechanisms. In Fig. 11 we present three cross-sections near Tocopilla, Taltal and La Ligua. In order to interpret our results it is necessary to define the top of the downgoing slap. Unfortunately, because of bad depth control, the Chilean Benioff zone is very poorly defined and we cannot use it as a marker of the top of the slab. For this reason, we made the hypothesis that the top of the slab is defined by the location of the trench and the hypocentres of the large underthrust events. These earthquakes occur at the interface between the two plates. The plate interface is well defined in the Taltal and La Ligua areas where the underthrust events (1966 December 28 and 1971 July 9) were rather large ($M_S > 7.5$) and had numerous aftershocks. The situation is less clear for the northernmost group because the 1967 December 21 earthquake, which was used to define the top of the slab, is relatively smaller and had very few aftershocks (Fig. 9). For lack of better data we shall retain the slab geometry defined in Fig. 11.

Our results indicate very clearly that extensional events occur inside the downgoing slab 20–30 km below the large interplate earthquakes. In our previous study of the La Ligua

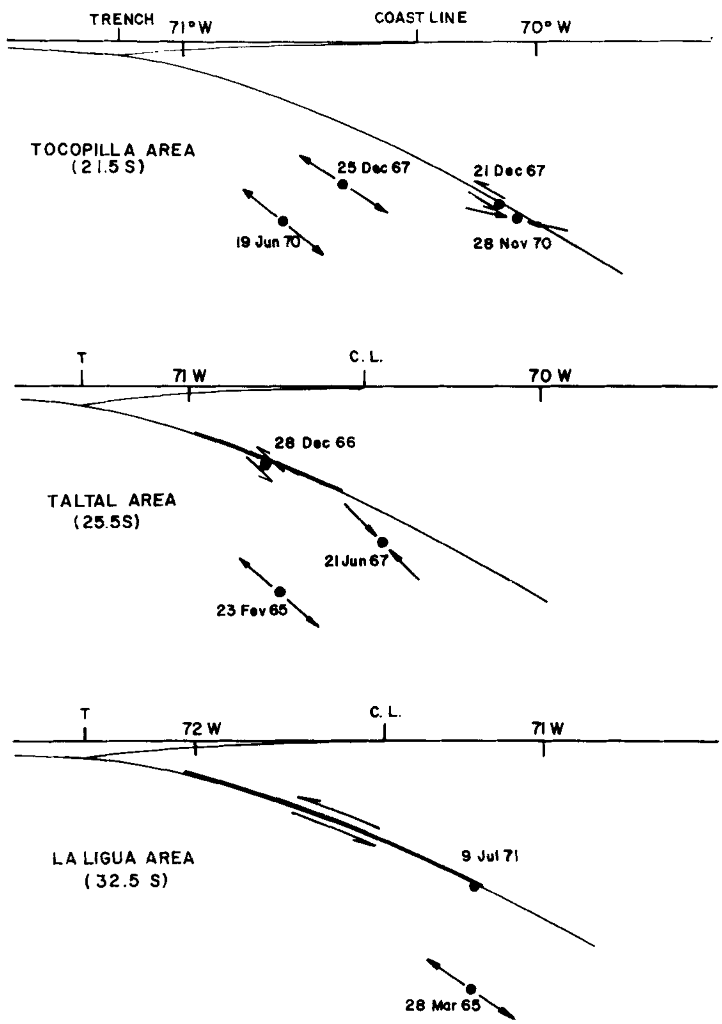

Figure 11. Cross-sections through the three areas of North-Central Chile discussed in the paper. The mechanisms of the earthquakes are indicated schematically. For intra-plate events we plot the tensional or compressional axis which is closer to the dip of the slab. For inter-plate events, we indicate the direction of slip on the fault plane determined from first motions. In the case of the 1966 December 28 earthquake in Taltal, the largest of those studied here, the first motions yield a fault plane which is too steep with respect to the Benioff zone.

earthquakes (Malgrange *et al.* 1981) we had interpreted the pair of events 5 and 12 in Fig. 1 with a model proposed by Abe (1972) for a similar pair of events off Central Peru in 1966 and 1970. In his model the shallow event was at the plate interface while the intermediate depth earthquake was due to slab pull. The results of the northern group show that these normal events occur *oceanwards* of the underthrust earthquakes. This would indicate the effect of slab pull is felt below the seismogenic zone at the plate interface.

The most interesting result of our study is that at least two compressional events have occurred near the plate interface, just below it in the Tocopilla and Taltal area. Extensive testing of the modelling of these events has convinced us that that these two events (1970 November 28 and 1967 June 21) are at least as deep as the large underthrust earthquakes at the plate interface. Thus, medium size ($M_s \sim 6$) compressional events occur occasionally near the top of the downgoing slab. The mechanisms of these two events are distinctly different of those of the underthrust events (compare, for instance, the mechanisms of Figs 5 and 8). The principal axes of the compressional earthquakes are rotated clockwise by 30° in the vertical plane with respect to those of the plate interface events.

Thus, we have found large shallow interplate events directly related to the subduction of the Nazca plate under South America; medium to large sized events some 30–40 km below the top of the downgoing slab due to extensional forces inside the slab; and, finally, smaller but well recorded compressional events on top of the downgoing slab. This situation is suggestive of the state of stress inferred for those regions where a double layered Benioff zone has been detected. There is at present no evidence of such a double layer at intermediate depths (70–180 km) in Chile. Thus, it appears that the mechanism which creates compression on top of the slab, whether by unbending (Engdahl & Scholz 1977), sagging (Yoshii 1979) or thermal stresses is more common than formerly thought.

Conclusion

This paper is a part of a systematic study of large Chilean earthquakes in order to understand a rather complex distribution of events with different fault plane solutions. A series of events were carefully studied by *P*-wave modelling and relative location techniques in order to improve fault plane solutions and hypocentral depth simultaneously. The results reveal a more complex pattern of fault plane solutions than originally expected. At two places we found relatively small events ($M \sim 6$) which had almost horizontal pressure axis and which occurred inside the downgoing slab near its upper surface. This is reminiscent of the double Benioff zones found under some island arcs, but we have no evidence of a double layer of events. The northern group of events, near 22°S, is particularly complex with a large $M = 7.4$ event which is probably an inter-plate earthquake; two normal fault events *oceanwards* of the large one and roughly at the same depth; and a horizontal compression earthquake, again at the same depth.

Acknowledgments

We are deeply indebted to Professor C. Lomnitz for his careful review of this work. The manuscript was greatly improved by the suggestions of two anonymous reviewers.

This work was supported by the Institut National d'Astronomie et Géophysique under ATP Géodynamique. Institut de Physique du Globe, contribution number 610.

References

Abe, K., 1972. Mechanisms and tectonic implications of the 1966 and 1970 Peru earthquakes, *Phys. Earth planet. Int.*, **5**, 367–379.

Barazangi, M. & Isacks, B. L., 1976. Spatial distribution of earthquakes and subduction of the Nazca plate beneath South America, *Geology*, **4**, 686–692.

Deschamps, A., Lyon-Caen, H. & Madariaga, R., 1980. Etude du tremblement de terre de Taltal (Chili 1966) à partir des ondes sismiques de longue période, *Annls Géophys.*, **36**, 179–190.

Engdahl, R. & Scholz, C. H., 1977. A double Benioff zone beneath the Central Aleutians, an unbending of the lithosphere, *Geophys. Res. Lett.*, **4**, 473–476.

Fitch, T. J., 1975. Compressional velocity in source regions of deep earthquakes: an application of the master event technique, *Earth planet. Sci. Lett.*, **26**, 156–166.

Fujita, K. & Kanamori, H., 1981. Double seismic zones and stresses of intermediate depth earthquakes, *Geophys. J. R. astr. Soc.*, **66**, 131–156.

Hanks, T. C., 1981. The corner frequency shift, earthquake source and *Q*, *Bull. seism. Soc. Am.*, **71**, 597–612.

Hanus, V. & Vanek, J., 1978. Morphology of the Andean Wadati–Benioff zone, andesitic volacanism, and tectonic features of the Nazca Plate, *Tectonophys.*, **44**, 65–77.

Hasegawa, A., Umino, N. & Takagi, A., 1978. Double-planed structure of the deep seismic zone in the northeastern Japan arc, *Tectonophys.*, **47**, 43–58.

Helmberger, D. V. & Langston, C. A., 1975. A procedure for modelling shallow dislocation sources, *Geophys. J. R. astr. Soc.*, **42**, 117–130.

Isacks, B. L. & Barazangi, M., 1977. Geometry of Benioff zones: lateral segmentation and downwards bending of the subducted lithosphere, in *Island Arcs, Deep Sea Trenchs and Back-arc Basins*, Ewing series, Vol. I, American Geophysical Union, Washington DC.

Isacks, B. & Molnar, P., 1971. Distribution of stresses in the descending lithosphere from a global survey of focal mechanism solutions of mantle earthquakes, *Rev. Geophys. Space Phys.*, **9**, 103–174.

Isacks, B. Oliver, J. & Sykes, L. R., 1968. Seismology and the new global tectonic, *J. geophys. Res.*, **73**, 5855–5899.

Kanamori, H., 1977. The energy release in great earthquakes, *J. geophys. Res.*, **82**, 2981–2987.

Kanamori, H. & Stewart, G., 1976. Mode of strain release along the Gibbs fracture zone, mid-Atlantic ridge, *Phys. Earth planet. Int.*, **11**, 312–332.

Kausel, E. & Lomnitz, C., 1968. Tectonics of Chile, in *Simposio Panamericano del Manto Superior*, Instituto de Geofisica, UNAM, Mexico.

Kelleher, J. A., 1972. Rupture zones of large South American earthquakes and some predictions, *J. geophys. Res.*, **77**, 2087–2103.

Lomnitz, C., 1970. Major earthquakes and tsunamis in Chile during the period 1535 to 1955, *Geol. Rdsch.*, **59**, 938–960.

Malgrange, M., 1981. Mécanismes et profondeurs de séismes du nord du Chili en relation avec l'état de contrainte de la plaque océanique de Nazca, *thèse*, Université Paris VII, France.

Malgrange, M., Deschamps, A. & Madariaga, R., 1981. Thrust and extensional faulting under the Chilean coast: 1965–1971 Aconcagua earthquakes, *Geophys. J. R. astr. Soc.*, **66**, 313–332.

McCann, W. R., Nishenko, S. P., Sykes, L. R. & Krause, J., 1979. Seismic gaps and plate tectonics: seismic potential for major boundaries, *Pageoph*, **117**, 1082–1147.

Pitt, A. M. & Ellis, J., 1968. Preliminary report on some aftershocks of the December 28, 1966 earthquake in Northern Chile, *Bull. seism. Soc. Am.*, **58**, 843–850.

Spence, W., 1980. Relative epicentre determination using *P*-wave arrival time differences, *Bull. seism. Soc. Am.*, **70**, 171–183.

Stauder, W., 1973. Mechanism and spatial distribution of Chilean earthquakes with relation to subduction of the oceanic plate, *J. geophys. Res.*, **78**, 5033–5061.

Stauder, W., 1975. Subduction of the Nazca plate under Peru as evidenced by focal mechanisms and by seismicity, *J. geophys. Res.*, **80**, 1053–1064.

Uyeda, S. & Kanamori, H., 1979. Back-arc opening and the mode of subduction, *J. geophys. Res.*, **84**, 1049–1061.

Yoshi, T., 1979. A detailed cross-section of the deep seismic zone beneath northeastern Honshu, Japan, *Tectonophys.*, **55**, 349–360.